POLISH MARITIME RESEARCH 2(78) 2013 Vol 20; pp. 61-66
10.2478/pomr-2013-0017

Numerical model to study the combustion process and emissions in the Wärtsilä 6L 46 four-stroke marine engine

Lamas, M. I., Assoc. Prof.
Rodríguez, C. G., M. Sc.
Escola Universitaria Politécnica. Universidade da Coruña, Spain

ABSTRACT

The aim of the present paper is to develop a computational fluid dynamics (CFD) analysis to study the combustion process in a four-stroke marine diesel engine, the Wärtsilä 6L 46*. The motivation comes from the importance of emissions from marine engines in the global emissions, particularly for nitrogen oxides (NO_x) and sulfur oxides (SO_x). The pressure and temperature fields were obtained, as well as the exhaust gas composition. In order to validate this work, the numerical results were satisfactory compared with experimental ones, which indicates that this model is accurate enough to reproduce the fluid pattern inside the cylinder during the combustion process. Accordingly, the aim of future works is to use this numerical procedure to optimize the performance and reduce the emissions of the new marine engine designs.*

Key words: Marine engine; emissions; combustion; CFD (Computational Fluid Dynamics)

INTRODUCTION

Nowadays, the world's ships are mainly powered by diesel engines. Marine diesel engines are very efficient, but they emit high levels of carbon dioxide (CO_2), nitrogen oxides (NO_x) and sulfur oxides (SO_x). Studies show that emissions of CO_2, NO_x and SO_x from ships correspond to about 2, 11 and 4% of the global anthropogenic emissions respectively (Skjřlsvik *et al*., 2000). Carbon dioxide is not toxic, but it contributes to the greenhouse effect (global warming)[1)]. It is the main greenhouse gas emitted by ships. Nitrogen oxides contribute significantly to the ozone layer depletion[2)]. They also form acids, which fall to earth as rain, fog, snow or dry particles, having harmful impacts on plants, animals and sea. Sulfur oxides, which are formed because of the high sulfur content of marine fuels (in order to reduce costs, ships generally use low quality fuels which tend to have a high sulfur content), are the major source of acid rain. To a lesser extent, other emissions from ships are carbon monoxide (CO), which is toxic to humans and animals; hydrocarbons, which contribute to the greenhouse effect and particulates, which can induce cardiopulmonary diseases and lung cancer. In harbour cities, emissions from ships constitute an important source of pollution. Furthermore, some gases may be transported in the atmosphere over several hundred of kilometers, contributing to air quality problems on land.

Merchant ships in international traffic are subjected to International Maritime Organization (IMO). In particular, the IMO Marpol Annex VI (Regulations for the Prevention of Air Pollution from Ships) limits SO_x and NO_x emissions from marine engines. As SO_x emissions are a function of the sulfur content of fuel, the IMO has limited the sulfur content in fuels. Concerning the NO_x, the IMO has established a curve which indicates the maximum allowable NO_x emission levels related to the engine speed. Figure 1 shows the maximum NO_x emission levels for marine diesel engines built after 2000 (IMO Tier I), 2011 (IMO Tier II) and 2016 (IMO Tier III, only in designated special areas called emission control areas). Apart from these international limitations, some regions have developed regional and national tougher limits.

Due to this legislation, the reduction of NO_x emissions is very important for the new marine engine designs. Several studies about NO_x emissions and other pollutants from marine engines can be found in the literature. For example, those of Li *et al.* [1], Lü *et al.* [2], Holub *et al.* [3], Jayaram *et al.* [4], Yan *et al*. [5], Uriondo *et al.* [6], Bernecic and Radonja [7], Maiboom and Tauzia [8], Duran *et al.* [9] and Millo *et al*. [10]. These

1) The greenhouse effect is a process by which thermal radiation from the planetary surface is absorbed by atmospheric greenhouse gases, which re-radiate part of this heat towards the surface again. As a result, the earth's temperature is higher than it would be if direct heating by solar radiation were the only warming mechanism.

2) The ozone layer is a deep layer in the stratosphere. It is composed by molecules of ozone, O_3, which filter out a lot of the sun's UV-B rays. Certain chemical substances can destroy some of the ozone, and the consequences are potentially damage to the life forms on Earth.

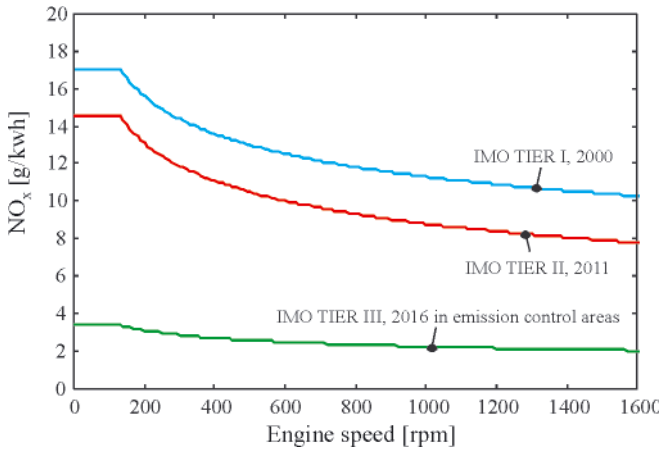

Fig. 1. *IMO maximum allowable NO_x emission for marine engines*

and other investigations have provided a great progress in the marine emission control technologies. However, the design of an efficient marine engine requires a complete understanding of the combustion process, which has a noticeably influence on the emissions. There are many possible combinations between the operating parameters (compression ratio, injection characteristics, combustion chamber geometry, etc), and the effects on the engine performance and emissions produced by variations of these parameters are non linear and often opposed. In this regard, CFD (Computational Fluid Dynamics) offers an important tool to study the fluid flow in detail. CFD is a branch of fluid mechanics based on the subdivision of the computational domain into small elements overlaying the whole domain. For each subdivision, the governing equations are solved using numerical methods.

This work proposes a CFD model to study the combustion process in the Wärtsilä 6L 46 four-stroke marine engine. The temperatures, pressures, advancing of the flame front and composition of the exhaust gas were obtained. The numerical model was validated with experimental measurements performed on a Wärtsilä 6L 46 installed on a tuna fishing vessel, obtaining a good agreement. This work is a continuation of Lamas *et al.* [11], in which the exhaust, intake and compression strokes of the cylinder operation were simulated.

CASE STUDIED

Technical specifications

The Wärtsilä 6L 46 studied in the present work is shown in Fig. 2. This is a four-stroke marine diesel engine with 6 cylinders in line, 46 cm bore, 58 cm stroke and 96400 cm^3 cylinder displacement volume. Each cylinder has two intake valves and two exhaust valves, and the fuel injector is placed at the center of the cylinder head. Figure 3 outlines a cross-section of the engine.

The present work was developed under the conditions studied in Lamas *et al.* [11]. These are 96% load, 499.6 rpm and employing heavy fuel oil (RMG 380 according to ISO 8217). Under these conditions, the power was 5212 kW and the consumption 172 g/kWh (9.96 g of fuel injected per cycle and cylinder). The in-cylinder gauge pressure is shown in Fig. 4, obtained using the engine performance analyzer MALIN 6000 (Malin Instruments, Ltd.).

Performance and combustion process

The performance of this engine was described in Lamas *et al.* [11], where it was explained that combustion takes place

Fig. 2. *Engine studied in the present work*

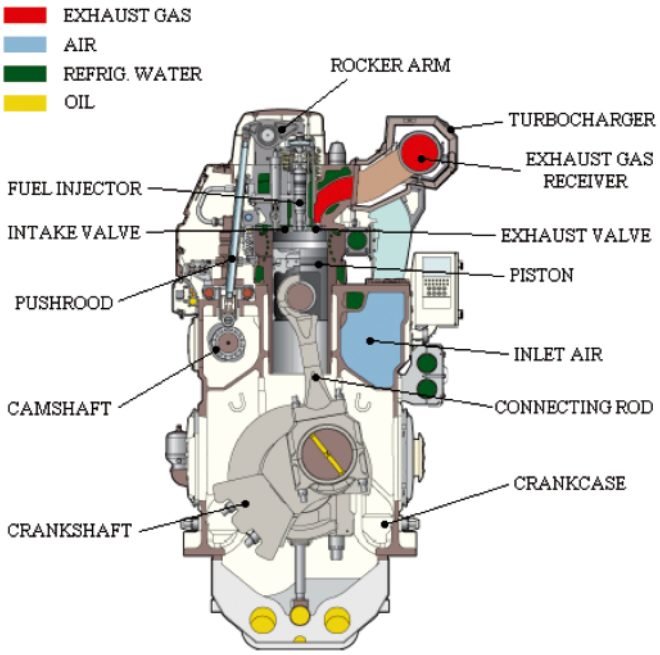

Fig. 3. *Cross section. Adapted from Wärtsilä [12]*

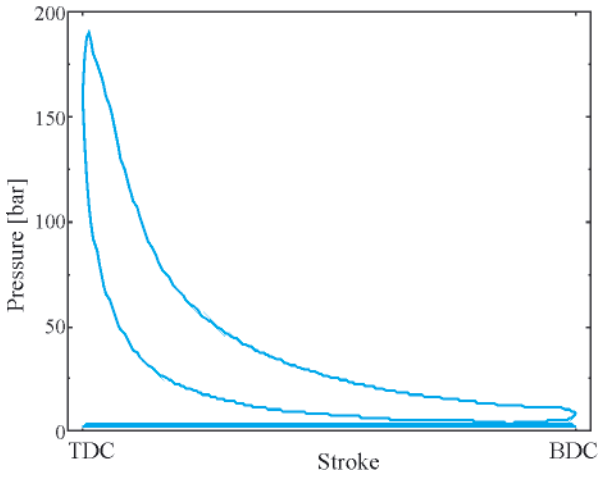

Fig. 4. *In-cylinder pressure experimentally measured*

towards the end of the compression stroke, with the piston near top dead center (TDC). As this is a direct injection engine, the fuel is injected directly into the combustion chamber. The combustion chamber is a shallow bowl in the piston crown shown in Fig. 5, which illustrates a photograph of three pistons of this engine.

Fig. 5. *Pistons of the engine studied in the present work*

The injection process is shown schematically in Fig. 6(a). The fuel is introduced by a 10 holes injector, Fig. 6(b), in the form of a spray of liquid droplets. As the air contained in the cylinder is at high pressure and temperature, the fuel vaporizes and mixes with this air. After that, ignition takes place. Atomization, vaporization, fuel-air mixing and combustion continue until all the necessary fuel has passed through each process. In addition, mixing of the air remaining in the cylinder with burning and already burned gas continues throughout the combustion and expansion processes.

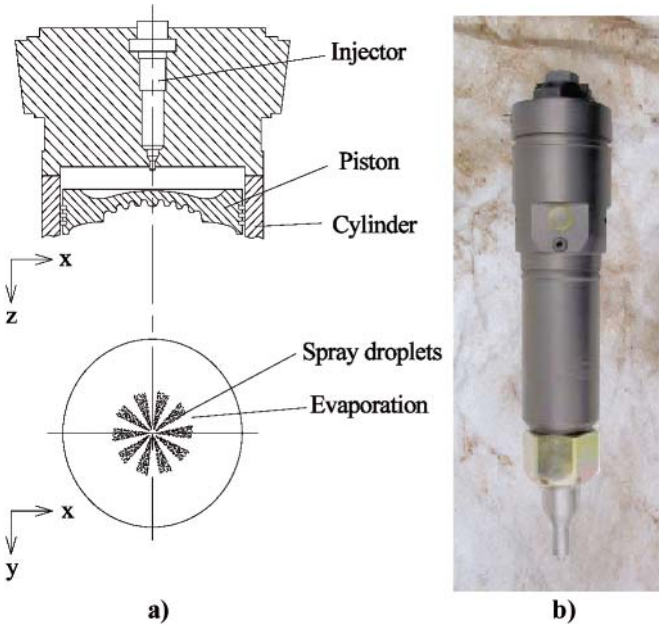

Fig. 6. a) *Schematic representation of the spray injection;* ***b)*** *photograph of the injector*

COMBUSTION CHEMISTRY AND GOVERNING EQUATIONS

Combustion is a very complex phenomenon which involves different disciplines such as fluid mechanics, chemistry, thermodynamics, heat transfer, etc. It is defined as an oxidation process of a fuel (in this case diesel, $C_{12}H_{23}$) and an oxidant (in this case oxygen, O_2), converting chemical energy into heat energy.

If a fuel is burnt stoichiometrically and ideally, this would be oxidized with air (which has a molecule of oxygen per 3.76 molecules of nitrogen) by means of the following reaction:

$$4C_{12}H_{23} + 71(O_2 + 3.76N_2) \rightarrow \rightarrow 48CO_2 + 46H_2O + 71 \cdot 3.76N_2 \quad (1)$$

This reaction is very simple because it only involves five chemical species, $C_{12}H_{23}$, O_2, N_2, CO_2 and H_2O and four elements, C, H, O and N. Unfortunately, this ideal mechanism never occurs and real combustion processes are governed by hundreds of reactions and tens of chemical species. Currently, there are no computational resources to model all the reactions and species involved in the combustion process. The solution is to simplify the physical phenomenon which governs the chemical reactions, explained in what follows.

Governing equations

In this engine, the cylinder is full of air before the injection of fuel, and combustion takes place as the fuel is being injected. This is known as non-premixed combustion (in contrast to premixed combustion, in which fuel and oxidant are mixed before combustion takes place). In non-premixed combustion, the rate of combustion is controlled by the rate at which fuel and air mix. Under such hypothesis, the equation which characterizes the propagation of the flame front is given by:

$$\frac{\partial}{\partial t}(\rho f) + \frac{\partial}{\partial x_i}(\rho u_i f) = \frac{\partial}{\partial x_i}\left(\frac{\mu_t}{\sigma_\xi}\frac{\partial f}{\partial x_i}\right) \quad (2)$$

where ρ is the density, σ_ξ the turbulent Schmidt number and f the mixture fraction. This is the local mass fraction of burnt and unburnt fuel stream elements (C, H, etc) in all the species (CO_2, H_2O, O_2, etc). For the following chemical reaction, in which C represents the fuel, O the oxidant and P the products:

$$cC + oO \rightarrow (c + o)P \quad (3)$$

the mixture fraction is given by:

$$f = c/(c + o) \quad (4)$$

In addition to this equation, the equations of conservation of mass, momentum and energy are also necessary, Eqs. (5) to (7) respectively:

$$\frac{\partial \rho}{\partial t} + \frac{\partial}{\partial x_i}(\rho u_i) = 0 \quad (5)$$

$$\frac{\partial}{\partial t}(\rho u_i) + \frac{\partial}{\partial x_j}(\rho u_i u_j) = = -\frac{\partial p}{\partial x_i} + \frac{\partial \tau_{ij}}{\partial x_j} + \frac{\partial}{\partial x_j}\left(-\rho \overline{u_i' u_j'}\right) \quad (6)$$

$$\frac{\partial}{\partial t}(\rho H) + \frac{\partial}{\partial x_i}(\rho u_i H) = = \frac{\partial}{\partial x_i}\left[\left(\frac{\mu}{\sigma} + \frac{\mu_t}{\sigma_h}\right)\frac{\partial H}{\partial x_i}\right] + S_{rad} \quad (7)$$

In the equations above, p is the pressure, τ_{ij} the viscous stress tensor, H the enthalpy, μ the, σ the Prandtl number, μ_t the turbulent viscosity, σ_h the turbulent Prandtl number and S_{rad} a source term to include the radiation heat transfer. The term

$-\rho\overline{u_i'u_j'}$ represents the Reynolds stresses, which were computed by means of the k-ε turbulence model.

Concerning the characterization of the chemical species involved, these were computed using the concept of chemical equilibrium (the chemical kinetics is so fast that equilibrium is reached quickly). The following 20 chemical species were considered: $C_{12}H_{23}$ (fuel), O_2, N_2, CO_2, H_2O, CO, C, CH_4, O, H, H_2, H_2O_2, N, OH, HO_2, HNO, HONO, C_2H_6, HCO and CHO.

NO_x is formed due to the high temperatures reached during the combustion process. Around 1500°C and above, enough thermal energy is available to dissociate oxygen and nitrogen, which recombine to form NO_x, Versteeg and Malalasekera [15]. NO_x emissions from ships are relatively high because most marine engines operate at high temperatures and pressures without effective NO_x reduction technologies. The reactions of formation of NO_x are not fast enough to consider chemical equilibrium. For this reason, its treatment was decoupled from the combustion model. Among the NO_x components, NO is the main pollutant (nearly 100% of NO_x is NO). NO is generated by the reactions proposed by Zeldovich [13], reactions (8) and (9), and Lavoie [14], reaction (10).

$$O + N_2 \overset{k_1}{\leftrightarrow} NO + N \tag{8}$$

$$N + O_2 \overset{k_2}{\leftrightarrow} NO + O \tag{9}$$

$$N + OH \overset{k_3}{\leftrightarrow} NO + H \tag{10}$$

The rate of formation of NO is given by the following expression:

$$\begin{aligned} d[NO]/dt &= k_1[O][N_2] + k_2[N][O_2] \\ &+ k_3[N][OH] - k_{-1}[NO][N] + \\ &- k_{-2}[NO][O] - k_{-3}[NO][H] \end{aligned} \tag{11}$$

where [NO], [O], [N_2], [N], [O_2], [OH] and [H] are the concentrations, mol/m³. k_1, k_2, k_3 are the rate constants and k_{-1}, k_{-2}, k_{-3} are the corresponding reverse rates. The forward and backward reaction rate constants for these three key reactions are given by:

$$\begin{aligned} k_1 &= 1.8x10^{11}e^{(-38370/T)} \\ k_2 &= 1.8x10^{7}Te^{(-4680/T)} \\ k_3 &= 7.1x10^{10}e^{(-450/T)} \\ k_{-1} &= 3.8x10^{10}e^{(-425/T)} \\ k_{-2} &= 3.8x10^{6}Te^{(-20820/T)} \\ k_{-3} &= 1.7x10^{11}e^{(-24560/T)} \end{aligned} \tag{12}$$

As can be seen, the reactions above are very dependent on the temperature. The NO formation rate is much slower than the combustion rate and most of the NO is formed after the completion of the combustion, due to the high temperatures present in the combustion zone.

NUMERICAL PROCEDURE

The numerical computations were performed by means of the commercial software ANSYS Fluent. It was carried out a period of time from 30° before TDC to the exhaust valves opening, 127° after TDC. All valves remained closed during the entire simulation. The results of Lamas et al. [11] were continued to 30° before TDC and employed as initial conditions of the present work. Concerning the boundary conditions, the heat transfer from the cylinder to the cooling water was modeled as a convection type:

$$q = h(T_{gas} - T_{water}) \tag{13}$$

where q is the heat transferred, T_{gas} is the in-cylinder temperature, T_{water} is the cooling water temperature (78°C) and h is the heat transfer coefficient, given by the following expression, Taylor [16]:

$$h = 10.4\ kb^{-1/4}\ (u_{piston}/v)^{3/4} \tag{14}$$

where b is the cylinder bore, k the thermal conductivity of the gas, u_{piston} the mean piston speed and ν the kinematic viscosity of the gas. Substituting values into the above equation yields h = 4151 W/m²K.

In order to model the movement of the piston, a moving grid was employed. Figure 7 shows the grid at the start of the simulation, 30° before TDC, and at TDC. As can be seen, only the combustion chamber was simulated.

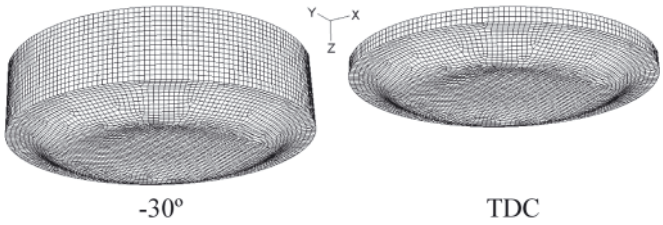

Fig. 7. Computational grid

RESULTS AND DISCUSSION

The spray and mass fraction of fuel are shown in Fig. 8. Under the conditions studied, the injection of fuel takes place from -12° to -1° crankshaft angles. Figure 8 represents -10°, -5° and 0° (PMS). As can be seen, the fuel spray enters the cylinder as liquid drops (which were simulated as 5 μm diameter). These

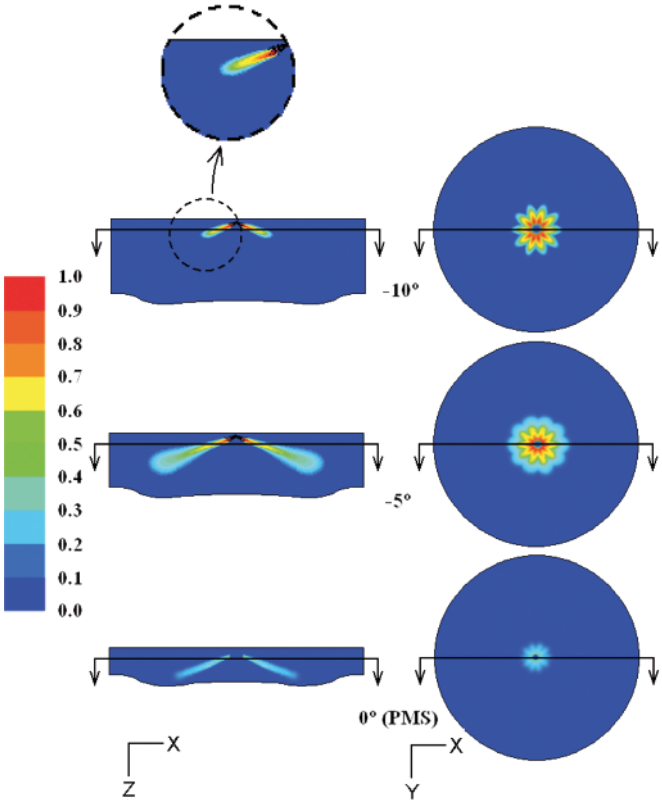

Fig. 8. Spray and mass fraction of fuel

drops are represented as black points in the figure. The structure of each fuel spray is that of a narrow liquid-containing core surrounded by a much larger gaseous-jet region containing fuel vapour. The flame spreads rapidly as the fuel is injected, producing a very fuel rich zone close to the fuel tip (-10° and -5°). After the injection of fuel has finished, the flame is extinguished progressively (0°).

The temperature field is shown in Fig. 9. The fuel is injected at 127°C, creating a cold temperature in the zone closed to the injector. In the rest of the cylinder, the temperature increases as the crankshaft angle is advanced due to the combustion progress and the compression supplied by the piston.

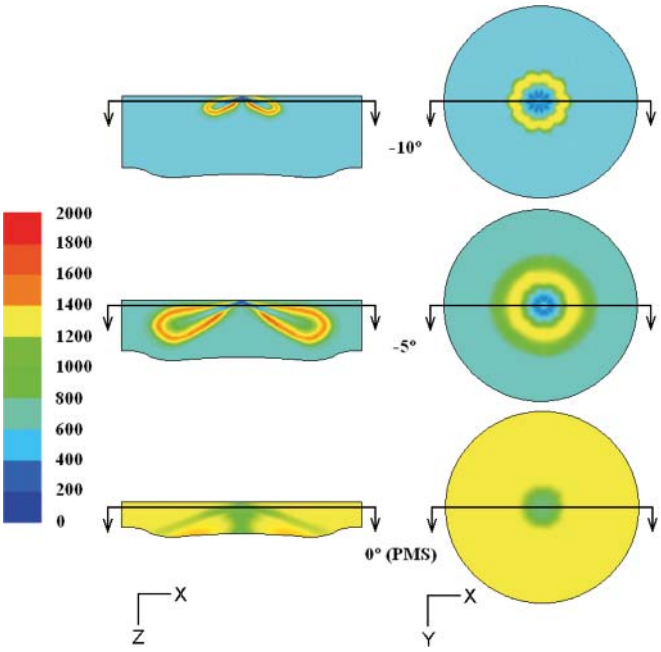

Fig. 9. *Temperature field (°C)*

Figure 10 illustrates the comparison of simulated and measured in-cylinder pressures. A satisfactory agreement between the experimental and numerical results was obtained.

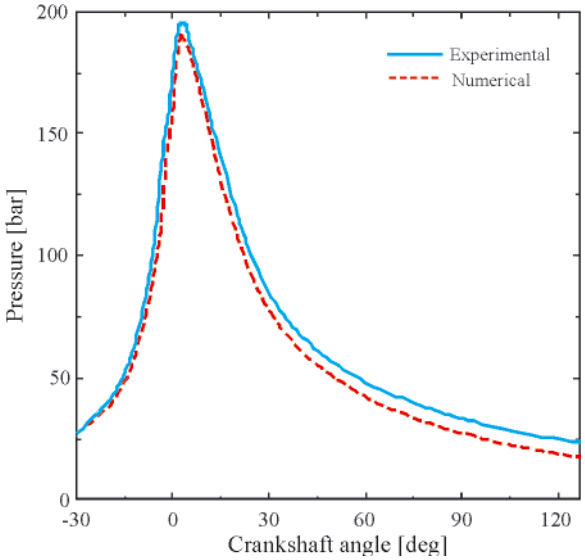

Fig. 10. *In-cylinder pressure numerically and experimentally obtained*

The emissions of carbon dioxide, carbon monoxide, nitrogen oxides and hydrocarbons are shown in Table 1. The NO_x emissions were measured experimentally using the G4100 analyzer (Green Instruments). According to this apparatus, the engine emits 1115 ppm of NO_x, which suppose an error of 13.8% with respect to the numerical result given in Table 1. This error is quite acceptable considering the difficulty of simulating the combustion process. As the CFD code provides the quantity of mass inside the cylinder, the NO_x emissions in g/kWh can be easily calculated, obtaining a value of 11.8. This value sticks the IMO TIER I but not IMO TIER II, applicable to engines mounted in vessels built after 1 January 2011. Several solutions to decrease the NO_x levels in this engine were proposed by Millo *et al.* [10].

Tab. 1. *Emissions from the engine numerically obtained*

Gas	CO_2 (% vol.)	CO (ppm* vol.)	NO_x (ppm vol.)	HC (ppm vol.)
Value	8.3	356	961	569

*ppm: parts per million

It is interesting to study the NO_x emissions against the start of injection (SOI). For the purpose, the SOI was varied between -13° and -10°. The experimental and numerical results are shown in Fig. 11. The peak pressures numerically and experimentally obtained are also shown in the figure. As can be seen, delaying the start of injection reduces the NO_x emissions and the peak pressure, both for the experimental and numerical results. The NO_x emissions are very sensitive to the temperature. The decrease in NOx emissions with injection retard is related to the decrease in combustion pressure and thus temperature. Unfortunately, the power is lower as the pressure decreases.

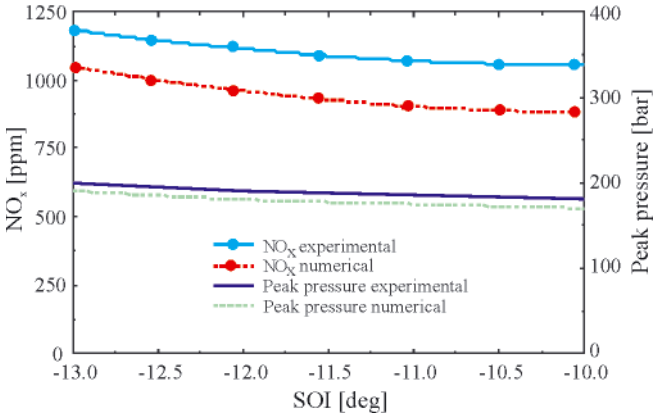

Fig. 11. *NOx emission varying with injection timing*

CONCLUSIONS AND FURTHER DEVELOPMENTS

The present paper proposes a CFD model to simulate the combustion process in the Wärtsilä 6L 46 marine engine. The strongest motivation is given by the current legislation, for which the most important gas component that must be reduced in exhaust emissions from marine engines is NO_x.

The pressure and temperature fields were obtained, as well as the composition of the exhaust gas. In order to validate this work, numerical results were satisfactory compared with experimental ones performed on a Wärtsilä 6L 46 installed on a tuna fishing vessel. This work provides a model to study several parameters such as injection pressure, compression ratio, injection timing, etc. In future works, the purpose is to employ this model to design low emission engines, analyzing measures such as water addition, retarded injection, modulated injection, exhaust gas recirculation, etc.

Acknowledgements

The authors would like to express their gratitude to "Talleres Pineiro, S.L.", marine engines maintenance and repair shop.

NOMENCLATURE

b – Cylinder bore
f – Mixture fraction
h – Heat transfer coefficient
H – Enthalpy
k – Thermal conductivity
p – Pressure
q – Heat transfer
t – Time
u – Velocity

Special characters

μ_t – Turbulent viscosity
ν – Kinematic viscosity
ρ – Density
σ_h – Turbulent Prandtl number
σ_ζ – Turbulent Schmidt number
τ_{ij} – Stress tensor

Subscripts

i – Cartesian coordinate (i = 1, 2, 3)
j – Cartesian coordinate (j = 1, 2, 3)

REFERENCES

1. Li, K; Li, B.; Sun, P.: *Influence of fuel injection advance angle on nitrogen oxide emission from marine diesel engine*. Journal of Dalian Maritime University 36(3), pp. 87-89, 2010.
2. Lü, L; Xu, J.H; Xu, W.Y.: *Effect of diesel oil quality on particulate and smoke emissions from marine diesel engine*. Chinese Internal Combustion Engine Engineering 31(4), pp. 44-48, 2010.
3. Holub, M.; Kalisiak, S.; Borkowski, T., Myskow, J; Brandenburg, R.: *The influence of direct non-thermal plasma treatment on particulate matter (PM) and NO_x in the exhaust of marine diesel engines*. Polish Journal of Environmental Studies 19(6), pp. 1199-1211, 2010.
4. Jayaram, V.; Nigam, A.; Welch, W.A.; Millar, J.W.; Cocker, I.I.: *Effectiveness of emission control technologies for auxiliary engines on ocean-going vessels*. Journal of the Air & Waste Management Association 61(1), pp. 14-21, 2011.
5. Yan, P; Feng, M.Z.; Ping, T.; Fang, W.C.; Wang, X.Q.: *Simulation research on effect of nozzle parameters on combustion and emissions for HPCR marine diesel engine*. Internal Combustion Engine Engineering 32(3), pp. 43-47, 2011.
6. Uriondo, Z.; Durán Grados, C.V.; Clemente, M.; Gutiérrez, J.M.; Martín, L.: *Effects of charged air temperature and pressure on NO_x emissions of marine medium speed engines*. Transportation research Part D: Transport and environment 16(4), pp. 288-295, 2011.
7. Bernecic, D.; Radonja, R.: *The selective catalytic reduction (SCR) application on two stroke slow speed marine diesel engines*. Pomorstvo 25(1), pp. 15-28, 2011.
8. Maiboom, A.; Tauzia, X. NO_x and PM emissions reduction on an automotive HSDI Diesel engine with water-in-diesel emulsion and EGR: An experimental study. *Fuel* 90(11), pp. 3179-3192, 2011.
9. Duran, V.; Uriondo, Z.; Moreno-Gutiérrez, J.: *The impact of marine engine operation and maintenance on emissions*. Transportation research Part D: Transport and environment 17(1), pp. 54 -60, 2012.
10. Millo, F.; Bernandi, M.G.; Delneri, D.: *Computational analysis of internal and external EGR strategies combined with miller cycle concept for a two-stage turbocharged medium speed marine diesel engine*. SAE Paper 2011-01-1141, 2011.
11. Lamas, M.I.; Rodríguez, C.G.; Rebollido, J.M.: *Numerical model to study the valve overlap period in the Wärtsilä 6L46 four-stroke marine engine*. Polish Maritime Research 1(72), pp. 31-37, 2012.
12. Wärtsilä 46: *Project guide for marine applications*. 2001.
13. Zeldovitch, Y.B.; Sadovnikov, D.A.; Kamenetskii, F.: *Oxidation of nitrogen in combustion*. Institute of Chemical Physics, Moscow-Leningrad, 1947.
14. Lavoie, G.A.; Heywood, J.B.; Keck, J.C.: *Experimental and theoretical investigation of nitric oxide formation in internal combustion engines*. Combustion Science Technology 1, pp. 313-326, 1970.
15. Versteeg H.K., Malalasekera W.: *An introduction to computational fluid dynamics: the finite volume method.* 2nd Edition. Harlow: Pearson Education, 2007.
16. Taylor, C.F.: *The internal combustion engine in theory and practice*. 2nd Edition. MIT Press, 1985.

CONTACT WITH THE AUTHORS

Lamas M. I., Assoc. Prof.
Rodríguez C. G., M. Sc.
Escola Universitaria Politécnica. Universidade da Coruña.
Avda. 19 de Febreiro s/n - 15405 Ferrol - A Coruña. SPAIN.
e-mail: isabellamas@udc.es